25th ABCM International Congress of Mechanical Engineering
October 20-25, 2019, Uberlândia, MG, Brazil

COB-2019-2301
COMPARING MONTE CARLO WITH DISCRETE ORDINATES METHOD FOR SILICA-CORE GOLD NANOSHELLS ASSISTED LASER PHOTOTHERMAL THERAPY

Anderson N. Sousa
André Maurente
Department of Mechanical Engineering, Federal University of Rio Grande do Norte (UFRN), Campus Universitário, Lagoa Nova, Natal 59072-970, RN, Brazil
sousa@tutamail.com, amaurente@gmail.com

Abstract. *Photothermal Therapy (PTT) uses electromagnetic radiation to increase tissue temperature and kill targeted cancerous cells. In this work, silica-core gold nanoshells are the photon absorbers that convert the electromagnetic energy into heat. The main objective is to compare Monte Carlo (MC) method with Discrete Ordinates (DO) method for the solution of the Radiative Transfer Equation (RTE) in an one-dimensional bioheat transfer model composed of five layers, one of them with a cancerous tumor and silica-core gold nanoparticles, irradiated by a near-infraed (NIR) laser. The overall maximum difference of peak temperature was equal to* $0.085053\ ^{\circ}C$ *at* $35\ s$ *of simulated time, and the maximum difference of tissue depth for peak temperature was equal to* $0.0125\ mm$*. Results demonstrated both methods performing similarly for this specific task.*

Keywords: *Monte Carlo simulation, Pennes equation, bioheat transfer, skin cancer, gold nanoparticles*

1. INTRODUCTION

The Photothermal Therapy (PTT) uses electromagnetic radiation to increase biological tissue temperature and damage cancerous cells by hyperthermia (Sheng *et al.*, 2017; Bayazitoglu *et al.*, 2013). In the present study, a near-infrared (NIR) laser targets silica-core gold nanoshells embedded in the tumor region, which are photon-absorbers capable of converting the irradiated laser energy into heat. The NIR laser can propagate into the human body without significant attenuation, as the extinction coefficient of most biological tissues is low for the *near-infrared window*, also known as *therapeutic window*, the range of wavelengths from 650 to 1350 nm (Smith *et al.*, 2009).

The development of the PTT demands an analysis of the propagation of light and heat in the biological tissue and their interaction with the nanoparticles and tissue structures. Theoretical studies improve the understatement of optical, electrodynamics, and heat transfer phenomena, consequently increasing the reliability of the technique. Numerical models use the bioheat transfer equation, first developed by Pennes (1948), to analyze the heat propagation in the modeled tissue. Ismailov *et al.* (2018), Malek and Abbasi (2016), and Sarkar (2017) present recent applications of the equation. Mesicek and Kuca (2018) developed a summary of numerical analyses for therapeutic uses of laser-activated gold nanoparticles and Manuchehrabadi and Zhu (2014) conducted an in-deep study of Monte Carlo method applied to the RTE coupled with the bioheat transfer equation in a prostate cancer model.

There are various groups of photon-absorbers, which one works with a specific source of energy (Sheng *et al.*, 2017; Bayazitoglu *et al.*, 2013). A gold nanoshell consists of a spherical core nanoparticle, such as silica or polystyrene, coated with a thin layer of gold (Abadeer and Murphy, 2016; Nghiem *et al.*, 2013; Liu and Li, 2013). The process that makes the conversion of electromagnetic energy into heat is named *surface plasmon resonance*, which can be fine tuned over the visible to NIR spectrum range by changing the core-shell diameter ratio (Vincenzo *et al.*, 2017; Nghiem *et al.*, 2013). In PTT, photon-absorbers delimit the region affected by hyperthermia. Mallory *et al.* (2016) and Cumming and Diamond (2002) detailed the biological mechanisms of hyperthermia in cancer treatments.

The present work is based on a model presented by Dombrovsky *et al.* (2011) to simulate the heat transfer phenomena occurring in a silica-core gold nanoshells assisted laser skin cancer photothermal therapy. One of the main difficulties is to find a solution for the RTE, as it requires integrals with angular and spatial variables. Our primary purpose is to compare Monte Carlo (MC) with Discrete Ordinates (DO) method for the solution of the radiative transfer equation (RTE) coupled

with other heat transfer phenomenons. The advantage of DO over MC is less processing time, although with MC is easier to simulate more complexities, such as anisotropic scattering and three-dimensional irregular geometries. (Maurente and França, 2015; Howell *et al.*, 2010).

2. MATHEMATICAL EQUATIONS AND MODELING

The study considered an one-dimensional model of a body tissue with skin cancer composed of five layers, one of them with a tumor and gold nanoshells, irradiated by a collimated laser.

2.1 The Pennes' bioheat trasnfer equation

The Pennes' equation is a well-known formula to calculate heat transfer in biological tissues (Pennes, 1948). The equation adds a blood perfusion term to the transient energy equation and it's necessary to calculate temperature distribution:

$$\rho c_p \frac{\delta T}{\delta t} = \nabla \cdot (\kappa \nabla T) + \nabla \cdot q_r + \rho_b v_b c_b \left(T_\mathrm{b} - T\right) \tag{1}$$

where ρ, c_p, T, t, and κ represents tissue density, specific heat, temperature, time and, conductivity, respectively. The second term on the right side accounts for the divergence of the heat flux. Finally, the last term includes blood perfusion in the equation, as b and v represent blood terms and perfusion rate, in that order.

Considering an one-dimensional model, the previous equation can be reduced to x direction, with $dq_{r,x}$ representing the radiative heat flux resultant of incident rays coming from all directions and crossing an element of area normal to the direction x:

$$\rho c_p \frac{\delta T}{\delta t} = \frac{d}{dx}\left(k \frac{T}{dx}\right) + \frac{dq_{r,x}}{dx} + \rho_b v_b c_b \left(T_b - T\right) \tag{2}$$

2.2 The Radiative Transfer Equation (RTE)

The following equations follow the procedures presented by Bruno *et al.* (2016). To find $dq_{r,x}$, one needs to solve the RTE, which returns the variation of the intensity of a radiation propagating in a direction s. For a quasi-steady configuration:

$$\frac{\mathrm{d}I_\lambda}{\mathrm{d}s} = \kappa_\lambda I_{\mathrm{bb},\lambda} - \beta_\lambda I_\lambda + \frac{\sigma_{\mathrm{sc},\lambda}}{4\pi} \int_{\Omega_i=0}^{4\pi} \Phi_\lambda\left(\Omega, \Omega_i\right) I_{\lambda,i}\left(\Omega_i\right) \mathrm{d}\Omega_i \tag{3}$$

where I is the radiation intensity, κ is the absorption coefficient, β is the extinction coefficient, σ_{sc} is scattering coefficient, and subscripts bb, i, and λ indicate black body, incident direction, and spectral dependency, respectively. $I_{\mathrm{bb},\lambda}$ is the resultant blackbody spectral intensity from the Plank function. Also, $\Phi_\lambda\left(\Omega, \Omega_i\right)$ is the scattering phase function, which accounts for the probability of a laser ray coming from a solid angle coordinate Ω_i be scattered into a solid angle coordinate Ω.

As the temperature to achieve hyperthermia is around $43°\mathrm{C}$ (Dickerson *et al.*, 2008), the emission of radiation from tissue is negligible when compared with the laser emission. Additionally, scattering was considered isoentropic ($\Phi_\lambda = 1$) and wavelength spectral dependence was unconsidered as a result of lasers being monochromatic. Adding the effects of the collimated irradiation in a source term, S_c, the resulting equations are:

$$\frac{dI}{ds} = -\beta I + \frac{\sigma_{sc}}{4\pi} \int_{\Omega_i=0}^{4\pi} I_i\left(\Omega_i\right) d\Omega_i + S_c \tag{4}$$

$$S_c = q_0 \frac{1}{4\pi}\left(1 - R_e\right) \exp\left(-\int_0^s \beta ds^*\right) \tag{5}$$

where, s is the depth of the irradiated surface, q_0 is the laser power, and R_e is the reflectivity of the external boundary surface, which is external to the tissue slab.

Finally, assuming surface emission as irrelevant and boundaries as gray and diffuse, with, $\hat{n}$ representing a unit vector outward to the surface, $\hat{s}$ a unit vector in the same direction as I_i, and S the surface boundary reflectivity, the boundary condition for Eq. (4) is:

$$I_w = q_0 \frac{1}{4\pi}\left(1 - R_e\right) + \frac{R}{\pi} \int_{\hat{n}\cdot\hat{s}<0} I_i\left(\Omega_i\right) |\hat{\mathbf{n}} \cdot \hat{\mathbf{s}}| d\Omega_i \tag{6}$$

As mentioned before, $dq_{r,x}$ is the resultant radiative heat flux generated by the incident rays coming from all directions and crossing an element of area normal to the direction x, therefore:

$$q_{r,x} = \int_{\Omega=0}^{4\pi} I(\Omega)\cos(\theta)\mathrm{d}\Omega \tag{7}$$

with θ being an angle referenced by x.

2.3 Spectral properties of human tissue with gold nanoshells

Considering a medium containing a limited volume fraction, f_v, of small spherical particles with the same radius a, absorption and scattering coefficients can be calculated with Eq. (8) and Eq. (9), respectively:

$$\kappa = \kappa_t + 0.75 f_v \frac{Q_a}{r} \tag{8}$$

$$\sigma_{sc} = \sigma_{sc,t} + 0.75 f_v \frac{Q_s}{r} \tag{9}$$

where t, f_v, Q_a, and Q_s represent tissue properties, volume fraction, absorption coefficient, and scattering coefficient, in that order (Dombrovsky *et al.*, 2011).

To solve the radiative transfer equation were applied two numerical methods, statistical Monte Carlo (MC) simulation and Discrete Ordinates (DO) with eighth order approximation for the angular discretzation, S_8. The codes were coupled with the same finite volume routine, based on Maliska (1995), which was used to solve the bioheat conduction and perfusion problems and to give the temperature distributions for the radiation, conduction and perfusion coupled model. The MC method followed the procedures presented by Maurente (2007), and the DO method was described by Modest (2013) and Howell *et al.* (2010). All the algorithms were implemented in *Fortran90*.

3. RESULTS AND DISCUSSION

The biological tissue model consists in a five-layer uni-dimensional geometry, which contains epidermis, tumor, papillary dermis, reticular dermis and fat. The presence of nanoparticles was considered in the first two layers, *epidermis* and *tumor*. "Fig. 1" displays a scheme of the model, and "Tab. 1" references the values used for tissue properties in each layer. In the model, the skin is irradiated by an helium-neon laser with an emissive power of $20\ \mathrm{kW/m^2}$ and wavelength equal to $0.6328\ \mu\mathrm{m}$, into the mentioned "therapeutic window".

Table 1. Biological tissue properties without nanoparticles (Dombrovsky *et al.*, 2011).

Tissue Layer	**Epidermis**	**Cancer tumor**	**Papilary dermis**	**Reticular dermis**	**Fat**
$\rho, \mathrm{kg/m^3}$	1200	1030	1200	1200	1000
$\mathrm{c_p, J/(kgK)}$	3589	3582	3300	3300	3674
$\mathrm{k, W/(mK)}$	0.235	0.558	0.445	0.445	0.185
$\dot{q}, \left(W/m^3\right)$	0	3680	368.1	368.1	368.3
$v_b, \left(kg/m^3\right)$	0	9.4	0.4	5.2	1
$\kappa, (m^-1)$	180	50	20	20	10
$\sigma_{sc}, \left(m^{-1}\right)$	2360	600	200	200	400

For "Eq. (2)" it was prescribed temperature of $37°\mathrm{C}$ on the left surface and convective heat transfer on the right with convective heat transfer coefficient equal to $h = 50\mathrm{W}/\left(\mathrm{m^2K}\right)$ for simulation of the heat transfer to inward biological tissues (Dombrovsky *et al.*, 2011).

Also, it was considered that the laser had been turned on during the first $10\ s$, then turned off during the next $15\ s$, then turned on again during the next $10\ s$ and, finally, turned off during the last $15\ s$, therefore totalling $50\ s$ of simulated time. Temperature distribution were plotted for 10, 25, 35, and $50\ s$ of simulated time, as shown on "Fig. 3".

As expected, "Fig. 3" illustrates a decreasing in overall temperature at $25\ s$ and $50\ s$, in agreement with the cooling due to the time which the laser was turned off. Because of the presence of nanoparticles in the region, epidermis and tumor, the temperature distribution shows its maximum at around $0.35\ mm$, and with a value high enough to kill cancerous

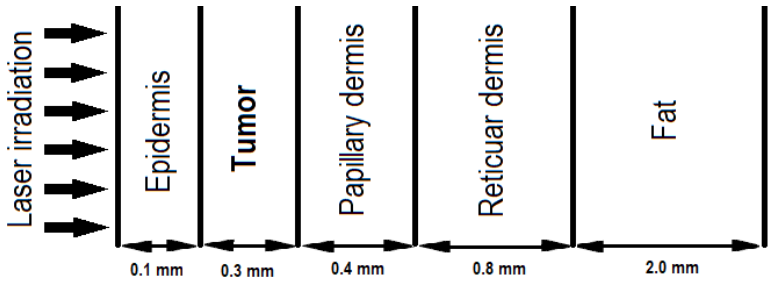

Figure 1. Biological tissue with skin cancer

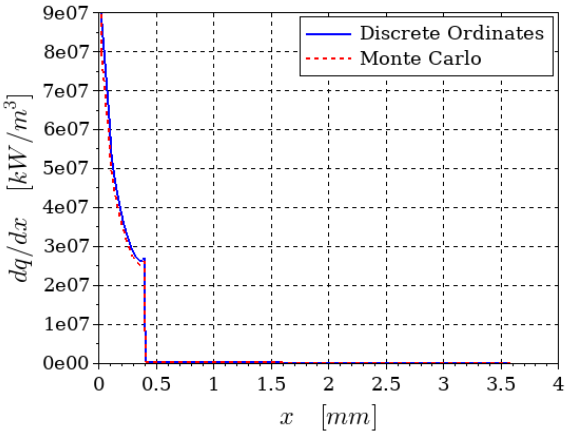

Figure 2. Divergence of the radiative heat flux

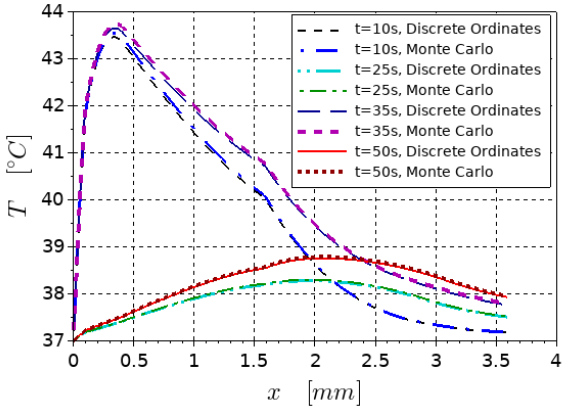

Figure 3. Temperature distribution at 10, 25, 35, and 50 s

tissue without damaging surrounding areas. Exact values of maximum temperatures are displayed in "Tab. 2", with the maximum overall temperature of 43.734436 °C at 35 s for Monte Carlo method and 43.649383 °C at 35 s for Discrete Ordinates. The maximum difference of peak temperature between the two methods was equal to 0.085053 and it occurs at the same time of maximum overall temperature, 35 s. Table shows bigger differences of maximum temperature to bigger values of maximum temperature. The depths of the peak temperatures had an excellent agreement between the two methods with the biggest difference being equal to only one step on the modeled depth vector, 0.0125 mm.

Additionally, "Fig. 2" represents the divergence of heat flux over time. Generally, both graphs shows the methods performing very similar. It's important to highlight that the presence of nanoparticles on the first two layers makes the absorption relatively irrelevant in the rest of the tissue, as can be observed in "Fig. 2".

Table 2. Maximum temperature and depth with max. temperature.

	Maximum temperature $(°C)$			**Depth with max. temperature** (mm)		
Time (s)	**Discrete Ordinates**	**Monte Carlo**	**Difference**	**Discrete Ordinates**	**Monte Carlo**	**Difference**
10	43.460999	43.540588	0.079589	0.340625	0.340625	0
25	38.27533	38.297058	0.021728	1.9656227	1.9656227	0
35	43.649383	43.734436	0.085053	0.340625	0.353125	0.0125
50	38.750427	38.782165	0.0317379	2.0781225	2.0656225	0.0125

The effects of the silica-core gold nanoshells were mathematically computed using "Eq. (8)" and "Eq. (9)", which changes the specific properties in the nanoparticles added layers. The radius of the nanoshells is $r = 20$ nm, and the radius of the silica-core is $0.75r$. Considering values of $Q_{\mathrm{a}} = 7.828$, $Q_{\mathrm{s}} = 1.144$, and $f_{\mathrm{v}} = 10^{-5}$ for the regions with nanoparticles, from "Eq. (8)" and "Eq. (9)" results are $\kappa = 3115.6\mathrm{m}^{-1}$ and $\sigma_{\mathrm{sc}} = 2789\mathrm{m}^{-1}$ for the epidermis, and $\kappa = 2985.5\mathrm{m}^{-1}$ and $\sigma_{\mathrm{sc}} = 1029\mathrm{m}^{-1}$ for the tumor. MC simulated an emission of 2000000 packs of energy, therefore, the results are associated with low statistical uncertainty.

4. CONCLUSION

Two methods for the solution of the radiative transfer equation in a one-dimensional model for silica-core gold nanoparticles assisted photothermal therapy were compared: Discrete Ordinates, with eighth order approximation for angular discretization, and Monte Carlo statistical method. Results show good agreement for temperature distribution and divergence of heat flux. The increasing and decreasing of temperature due laser being turned on and turned off, and the absorption effect generated by the presence of nanoparticles in the first two layers were well illustrated by the results. The overall maximum difference of peak temperature was equal to 0.085053 at $35\ s$, and the maximum depth difference of peak temperature was equal to $0.0125\ mm$.

The comparison between the two methods results allow to conclude that the discrete ordinate method was almost as accurate as the benchmark Monte Carlo method to calculate the divergent of the radiative heat flux and the radiative heat flux for predicting the temperature distributions in the considered problem. For future works, we suggest to test other conditions, which includes multidimensional geometry and anisotropic scattering in order to verify if the faster Discrete Ordinates method can handle such complexities.

5. ACKNOWLEDGEMENTS

The authors thank Coordenação de Aperfeiçoamento de Pessoal de Nível Superior (CAPES, Coordination for the Improvement of Higher Education Personnel) for the financial support.

6. REFERENCES

Abadeer, N.S. and Murphy, C.J., 2016. "Recent Progress in Cancer Thermal Therapy Using Gold Nanoparticles". *Journal of Physical Chemistry C*, Vol. 120, No. 9, pp. 4691–4716. ISSN 19327455. doi:10.1021/acs.jpcc.5b11232.

Bayazitoglu, Y., Kheradmand, S. and Tullius, T.K., 2013. "An overview of nanoparticle assisted laser therapy". *International Journal of Heat and Mass Transfer*, Vol. 67, pp. 469–486. ISSN 0017-9310. doi: 10.1016/j.ijheatmasstransfer.2013.08.018.

Bruno, A.B., Maurente, A., Lamien, B. and Orlande, H.R., 2016. "Numerical simulation of nanoparticles assisted laser photothermal therapy: a comparison of the P1-approximation and discrete ordinate methods". *Journal of the Brazilian Society of Mechanical Sciences and Engineering*, Vol. 39, No. 2, pp. 621–630. ISSN 18063691. doi:10.1007/s40430-016-0553-3.

Cumming, E.E. and Diamond, A.W., 2002. "The cellular and molecular basis of hyperthermia". *Canadian Field-Naturalist*, Vol. 116, No. 1, pp. 69–75. ISSN 00083550.

Dickerson, E.B., Dreaden, E.C., Huang, X., El-Sayed, I.H., Chu, H., Pushpanketh, S., McDonald, J.F. and El-Sayed, M.A., 2008. "Gold nanorod assisted near-infrared plasmonic photothermal therapy (PPTT) of squamous cell carcinoma in mice". *Cancer Letters*, Vol. 269, No. 1, pp. 57–66. ISSN 03043835. doi:10.1016/j.canlet.2008.04.026.

Dombrovsky, L.A., Timchenko, V., Jackson, M. and Yeoh, G.H., 2011. "International Journal of Heat and Mass Transfer A combined transient thermal model for laser hyperthermia of tumors with embedded gold nanoshells". *International Journal of Heat and Mass Transfer*, Vol. 54, No. 25-26, pp. 5459–5469. ISSN 0017-9310. doi: 10.1016/j.ijheatmasstransfer.2011.07.045.

Howell, J.R., Siegel, R. and Mengüç, M.P., 2010. *Thermal Radiation Heat Trasnfer*. CRC Press, fifith edition. ISBN 978-1-4398-9455-2.

Ismailov, M.I., Bazán, F.S. and Bedin, L., 2018. "Time-dependent perfusion coefficient estimation in a bioheat transfer problem". *Computer Physics Communications*, Vol. 230, pp. 50–58. ISSN 00104655. doi:10.1016/j.cpc.2018.04.019.

Liu, C. and Li, B., 2013. "Energy Absorption in Gold Nanoshells". *Journal of Nano Research*, Vol. 23, pp. 74–82. doi:10.4028/www.scientific.net/jnanor.23.74.

Malek, A. and Abbasi, G., 2016. "Optimal Control for Pennes' Bioheat Equation". *Asian Journal of Control*, Vol. 18, No. 2, pp. 674–685. ISSN 19346093. doi:10.1002/asjc.1059.

Maliska, C.R., 1995. *Transferncia de calor e mecnica dos fluidos computacional*.

Mallory, M., Gogineni, E., Jones, G.C., Greer, L. and Simone, C.B., 2016. "Therapeutic hyperthermia: The old, the new, and the upcoming". *Critical Reviews in Oncology/Hematology*, Vol. 97, No. 2015, pp. 56–64. ISSN 18790461. doi:10.1016/j.critrevonc.2015.08.003.

Manuchehrabadi, N. and Zhu, L., 2014. "Development of a computational simulation tool to design a protocol for treating prostate tumours using transurethral laser photothermal therapy". *International Journal of Hyperthermia*, Vol. 30, No. 6, pp. 349–361. ISSN 14645157. doi:10.3109/02656736.2014.948497.

Maurente, A., 2007. *Método de Monte Carlo aplicado ao modelamento espectral de meios participantes através da utilização da função de distribuição de energia de corpo negro nas linhas de absorção*. Ph.D. thesis, Universidade Federal do Rio Grande do Sul.

Maurente, A. and França, F.H., 2015. "A Multi-Spectral Energy Bundle method for efficient Monte Carlo radiation heat transfer computations in participating media". *International Journal of Heat and Mass Transfer*, Vol. 90, pp. 351–357. ISSN 00179310. doi:10.1016/j.ijheatmasstransfer.2015.06.067.

Mesicek, J. and Kuca, K., 2018. "Summary of numerical analyses for therapeutic uses of laser-activated gold nanoparticles". *International Journal of Hyperthermia*, Vol. 34, No. 8, pp. 1255–1264. ISSN 14645157. doi: 10.1080/02656736.2018.1440016.

Modest, M.F., 2013. *Radiative heat transfer*. Elsevier, 3rd edition. ISBN 978-0-12-386944-9.

Nghiem, T.H.L., Le, T.N., Do, T.H., Vu, T.T.D., Do, Q.H. and Tran, H.N., 2013. "Preparation and characterization of silica-gold core-shell nanoparticles". *Journal of Nanoparticle Research*, Vol. 15, No. 11. ISSN 13880764. doi: 10.1007/s11051-013-2091-6.

Pennes, H.H., 1948. "Analysis of tissue and arterial blood temperatures in the resting human forearm". *Journal of applied physiology (Bethesda, Md. : 1985)*, Vol. 1, No. 2, pp. 5–34. ISSN 8750-7587.

Sarkar, N., 2017. "A novel Pennes' bioheat transfer equation with memory-dependent derivative". *Mathematical Models in Engineering*, Vol. 2, No. 2, pp. 151–157. ISSN 2351-5279. doi:10.21595/mme.2016.18024.

Sheng, W., He, S., Seare, W.J. and Almutairi, A., 2017. "Review of the progress toward achieving heat confinement—the holy grail of photothermal therapy". *Journal of Biomedical Optics*, Vol. 22, No. 8, p. 080901. ISSN 1083-3668. doi:10.1117/1.jbo.22.8.080901.

Smith, A.M., Mancini, M.C. and Nie, S., 2009. "Bioimaging: Second window for in vivo imaging". *Nature Nanotechnology*, Vol. 4, No. 11, pp. 710–711. ISSN 17483395. doi:10.1038/nnano.2009.326.

Vincenzo, A., Roberto, P., Marco, F., Onofrio, M.M. and Maria Antonia, I., 2017. "Surface plasmon resonance in gold nanoparticles: a review". *Journal of Physics: Condensed Matter*, Vol. 29, No. 20, p. 203002.

7. RESPONSIBILITY NOTICE

The authors are the only responsible for the printed material included in this paper.